Lithuanian Journal of Physics
Vol. **64**, No. 3, pp. 162–176 (2024)
ISSN 1648-8504 eISSN 2424-3647
DOI: https://doi.org/10.3952/physics.2024.64.3.2

APPLICATION OF THE FROZEN-MODES APPROXIMATION TO CLASSICAL HARMONIC OSCILLATOR SYSTEMS

J. Vaičaitytė [a, b], L. Valkunas [a], and A. Gelzinis [a, b]

[a] *Department of Molecular Compound Physics, Center for Physical Sciences and Technology, Saulėtekio 3, 10257 Vilnius, Lithuania*

[b] *Institute of Chemical Physics, Faculty of Physics, Vilnius University, Saulėtekio 9, 10222 Vilnius, Lithuania*

Email: andrius.gelzinis@ftmc.lt

Received 2 April 2024; revised 6 May 2024; accepted 10 May 2024

The problems of open classical systems usually correspond to a motion of a test particle that interacts with a large number of bath oscillators. Often, the test particle itself can be considered a harmonic oscillator. For such composite systems, exact numerical solutions are available, but they can become increasingly costly for a large number of bath oscillators. Here we take inspiration from the recent work on open quantum systems and investigate the applicability of the frozen-modes approximation to such classical systems. This approach assumes that some part of the low-frequency bath modes are frozen, thus only their initial values need to be considered. We show that by applying the frozen-modes approximation one can significantly increase the accuracy of the perturbative multiple-scales solution, especially for slow baths. This approach provides a good accuracy even for strong system–bath couplings, a regime that is not accessible to straightforward applications of the perturbation theory. We also suggest a rule for the splitting of spectral density to the fast and slow bath modes. We find that our approach gives excellent results for the ohmic spectral density, but it could be applied for other similar spectral densities as well.

Keywords: classical oscillators, multiple-scales method, frozen modes

1. Introduction

Open systems constitute one of the cornerstones of modern physics. Though it is open *quantum* systems that are often in the forefront of the current research [1–3], open *classical* systems remain relevant to this day [4]. This is because the classical description is accurate enough for a large number of problems and, additionally, it is sometimes the only description feasible for larger systems. Indeed, classical mechanics is the foundation for molecular dynamics simulations [5]. In addition, classical treatment can give identical results to quantum treatment for some problems considering a molecule interacting with a solvent [6].

In typical problems of open classical systems, a test particle moving in some potential $V(X)$ is assumed to interact with an infinite set of harmonic oscillators, which constitute the environment. The test particle is then considered the system of interest. In some cases, more than one test particle is considered [7]. Usually, the entire supersystem (system+bath) is described by the Caldeira–Leggett [8] or the Ford–Kac [9] models. The choice of $V(X)$ depends on the problem under consideration.

Often the system of interest can also be considered as a harmonic oscillator [6, 7, 10]. Remarkably, it has been demonstrated that quantum states can be mapped to classical harmonic oscillators [11, 12]. In addition, it has been shown that a classical model reproduces many qualitative features of a quantum description for energy transfer problems [13].

For a composite system of coupled harmonic oscillators, an exact solution is available by transforming the problem to the normal mode representation. In such a case, the bath is described by a finite number of oscillators. For larger baths, however, diagonalization of the relevant matrices leads to a prohibitive computational cost.

Therefore, a straightforward numerical solution of the systems of ordinary differential equations is often performed instead, using Runge–Kutta or similar methods. Even so, calculations for very large baths (hundreds of oscillators) become expensive. For this reason, it is worthwhile to investigate approximate methods that could provide good accuracy at a fraction of the computational cost, at least for some parameter regimes.

In the case of open quantum systems, a very interesting theoretical approach was proposed in Ref. [14]. It was shown in that work that freezing some of the bath modes, i.e. disregarding their dynamical evolution, could lead to a significantly increased range of validity for a second-order quantum master equation. Such an approach then involves sampling the initial conditions of the frozen modes by a Monte-Carlo (MC) procedure, which is trivially parallelizable. In this way, the couplings of the frozen modes to the system of interest are taken into account non-perturbatively. Later, similar ideas were utilized for simulations of linear and nonlinear optical spectra [15]. More recently, the frozen-modes approximation was used to increase the applicability of the small polaron quantum master equation [16]. Here we take inspiration from these works and apply the frozen-modes approximation to the case of a classical system. We present a detailed theoretical framework that combines the perturbative method of multiple scales with the frozen-modes approximation. Our numerical investigations show that application of the frozen-modes approach can significantly increase the accuracy of the perturbative solution even for strong system–bath couplings. This approach is especially useful for slow baths, but can be beneficial for faster baths as well.

2. Methods

In this work, we consider a case where the main (system) oscillator is coupled to a large number of bath oscillators. The composite system is described by the Hamiltonian of Caldeira–Leggett type [8]:

$$\bar{H} = \frac{\bar{P}^2}{2M} + \frac{1}{2} M\Omega^2 \bar{X}^2 + \\ + \sum_{j=1}^{N} \left\{ \frac{\bar{p}_j^2}{2m_j} + \frac{1}{2} m_j \bar{\omega}_j^2 \left(\bar{x}_j - \frac{c_j \bar{X}}{m_j \bar{\omega}_j^2} \right)^2 \right\}. \tag{1}$$

Here $(\bar{P}, \bar{X})$ denote the momentum and the coordinate of the main oscillator with frequency Ω and mass M, while $(\bar{p}_j, \bar{x}_j)$ denote the momenta and the coordinates of the bath oscillators that interact with the main oscillator. The masses and frequencies of the bath modes are m_j and $\bar{\omega}_j$, respectively. The parameters c_j are the interaction coefficients between the main oscillator and the bath modes. The number of bath modes is N. To simplify the theoretical description, we hereafter switch to dimensionless variables: $P = \bar{P} / \sqrt{M\Omega\hbar}$, $X = \bar{X} / \sqrt{M\Omega / \hbar}$, $p_j = \bar{p}_j / \sqrt{m_j \bar{\omega}_j \hbar}$, $x_j = \bar{x}_j \sqrt{m_j \bar{\omega}_j / \hbar}$, $d_j = c_j \sqrt{m_j \bar{\omega}_j^3 M\Omega}$, $\omega_j = \bar{\omega}_j / \Omega$, $\tau = \Omega t$.

We further assume that the distribution of the couplings with the bath is determined by the dimensionless spectral density function, which is defined as

$$I(\omega) = \frac{\pi}{2} \sum_{j=1}^{N} \omega_j^2 d_j^2 \delta(\omega - \omega_j). \tag{2}$$

Here we will mostly consider the ohmic spectral density with the exponential cut-off,

$$I(\omega) = \frac{\lambda \pi \omega}{\omega_c} \exp\left(-\frac{\omega}{\omega_c} \right), \tag{3}$$

where $\lambda = \sum_{j=1}^{N} \frac{\omega_j d_j^2}{2} = \int_0^\infty \mathrm{d}\omega I(\omega) / (\pi\omega)$ is the dimensionless reorganization energy that defines the overall coupling strength between the system and the bath, and ω_c is the cut-off frequency. Such type of spectral density is widely used in the simulations of open quantum systems [17–20].

After having switched to non-dimensional variables and parameters, the dimensionless Hamiltonian, defined as $H = \bar{H} / (\hbar\Omega)$, is expressed in the following way:

$$H = \frac{1}{2}(P^2 + X^2) + \sum_{j=1}^{N} \frac{1}{2} \omega_j (p_j^2 + x_j^2) - \\ - \sum_{j=1}^{N} \omega_j d_j x_j X + \sum_{j=1}^{N} \frac{1}{2} \omega_j d_j^2 X^2. \tag{4}$$

Hamilton's equations are given by $\frac{\mathrm{d}p_j}{\mathrm{d}\tau} = -\frac{\partial H}{\partial x_j}, \frac{\mathrm{d}x_j}{\mathrm{d}\tau} = \frac{\partial H}{\partial p_j}$, therefore, the following system of equations is obtained:

$$\begin{cases} \ddot{X}+X+\sum_{j=1}^{N} d_j^2\omega_j X-\sum_{j=1}^{N} d_j\omega_j x_j=0; \\ \ddot{x}_j+\omega_j^2 x_j-d_j\omega_j^2 X=0. \end{cases} \tag{5}$$

Here dots denote the full derivative with respect to the dimensionless time τ. We suppose that the initial conditions are the following: $X(0) = X_0$, $P(0) = 0$, $x_j\ (0) = x_{j0}$, $p_j\ (0) = p_{j0}$. We will be interested in the mean squared displacement for the main oscillator, $\langle D(\tau)\rangle = \langle (X(\tau) - X_0)^2\rangle$, with averaging done over the initial conditions of the bath oscillators.

Assuming that the interaction coefficients are small, in other words, supposing that there is a small parameter $\varepsilon \ll 1$ next to d_j, we use perturbation theory to solve the system of equations given in Eq. (5). Perturbation theory is a method for solving problems that is based on the expansion of the desired solution in terms of a power series in a small parameter. In our case, we want to find an expression for the coordinate of the main oscillator as $X(\tau) = X^{(0)}\ (\tau) + \varepsilon X^{(1)}\ (\tau)$. As a result, the following expression is obtained:

$$\begin{aligned} X(\tau) &= \left(X_0 - \sum_{j=1}^{N} \frac{d_j\omega_j x_{j0}}{1-\omega_j^2} \right)\cos\tau + \\ &+ \sum_{j=1}^{N} \frac{d_j\omega_j^2 p_{j0}}{\omega_j^2-1}\sin\tau + \\ &+ \sum_{j=1}^{N} \frac{d_j\omega_j}{1-\omega_j^2}(x_{j0}\cos\omega_j\tau + p_{j0}\sin\omega_j\tau). \end{aligned} \tag{6}$$

Note that here and in all the solutions presented later we immediately set back $\varepsilon = 1$. In order to achieve more accurate results, the second-order solution for $X(\tau)$ can be obtained:

$$\begin{aligned} X(\tau) &= A\cos\tau + B\sin\tau + \\ &+ \sum_{j=1}^{N} \frac{d_j\omega_j}{1-\omega_j^2}(C_j\cos\omega_j\tau + D_j\sin\omega_j\tau) \\ &+ \frac{1}{2}\sum_{j=1}^{N} \frac{d_j^2\omega_j}{\omega_j^2-1}(-B\tau\cos\omega_j\tau + A\tau\sin\omega_j\tau). \end{aligned} \tag{7}$$

Here A, B, C_j and D_j are constants that can be determined using the initial conditions of the problem. However, terms multiplied by τ appear in the second-order solution. Thus, for larger values of τ, the solution increases without a bound, which is an unphysical result. This means that the perturbation theory has a rather limited range of validity for this problem.

As a consequence, we chose to use the multiple scales method to find $X(\tau)$ instead of the regular perturbation theory. The multiple scales method is a technique used to construct approximate solutions for perturbation problems, in which the solutions depend simultaneously on widely different scales 21–23]. For a considered oscillator system, we can expect that one scale would be related to the frequency of the unperturbed main oscillator, while another scale would correspond to the frequency shift due to the interaction with the bath. In order to find the second-order solution for $X(\tau)$, we postulated three time scales: $\tau_0 = \tau$, $\tau_1 = \varepsilon\tau$, $\tau_2 = \varepsilon^2\tau$. We assumed that a solution we are looking for is of the form $X = X^{(0)}\ (\tau_0, \tau_1, \tau_2) + \varepsilon X^{(1)}\ (\tau_0, \tau_1, \tau_2) + \varepsilon^2 X^{(2)}\ (\tau_0, \tau_1, \tau_2)$. This approach results in the solution for the system of equations given in Eq. (5) that is not unique. This implies that more conditions have to be imposed to completely determine the solution. This freedom allows us to prevent the occurrence of the linearly increasing secular terms. The resulting solution reads as

$$\begin{aligned} X(\tau) &= \left(X_0 - \sum_{j=1}^{N} \frac{d_j\omega_j x_{j0}}{1-\omega_j^2} - \sum_{j=1}^{N} \frac{d_j^2\omega_j^3 X_0}{(1-\omega_j^2)^2} \right)\times \\ &\times\cos\left(\sum_{j=1}^{N} \frac{d_j^2\omega_j\tau}{2(1-\omega_j^2)} + \tau \right) - \\ &- \sum_{j=1}^{N} \frac{d_j\omega_j^2 p_{j0}}{1-\omega_j^2}\sin\left(\sum_{j=1}^{N} \frac{d_j^2\omega_j\tau}{2(1-\omega_j^2)} + \tau \right) + \\ &+ \sum_{j=1}^{N} d_j\omega_j p_{j0}\sin\left(\omega_j\tau - \frac{d_j^2\omega_j^2\tau}{2(1-\omega_j^2)} \right) + \\ &+ \sum_{j=1}^{N} \frac{d_j\omega_j[(1-\omega_j^2)x_{j0} + d_j\omega_j^2 X_0]}{(1-\omega_j^2)^2}\cos\left(\omega_j\tau - \frac{d_j^2\omega_j^2\tau}{2(1-\omega_j^2)} \right). \end{aligned} \tag{8}$$

This expression can be used for calculations. It is desirable, however, to express the final answer in terms of integrals over the spectral density function. To this end, further approximations were made. First of all, it was assumed that $\omega_j \ll 1$. This essentially means that the frequency of the system oscillator is much greater than the frequencies of the bath modes. Thus, the terms in which $1 - \omega_j^2$ appear, ω_j^2 was neglected. This approximation is necessary in order

to avoid divergence when $\omega_j \to 1$. Additionally, the term $\omega_j\tau - \frac{d_j^2\omega_j^2\tau}{2(1-\omega_j^2)}$ that appears in sin and cos arguments was simplified in the following way:

$$\omega_j\tau - \frac{d_j^2\omega_j^2\tau}{2(1-\omega_j^2)} \approx \omega_j\tau - \frac{d_j^2\omega_j^2\tau}{2} = \omega_j\tau\left(1-\frac{d_j^2\omega_j}{2}\right) \approx \omega_j\tau.$$

Here $\frac{d_j^2\omega_j}{2}$ was neglected since it is assumed that $d_j \ll 1$ and $\omega_j \ll 1$, which makes the term $d_j^2\omega_j/2$ much smaller than 1. However, it was only neglected in sin and cos arguments as it prevents us from writing the final expression in terms of integrals. The sum of these small terms $\sum_{j=1}^{N}\frac{d_j^2\omega_j}{2}$ was kept elsewhere since it can be expressed as $\int_0^\infty \mathrm{d}\omega\, I(\omega)/(\pi\omega)$, and is, in fact, the reorganization energy of the system. After applying these approximations, the expression of $X(\tau)$ turns to

$$\begin{aligned} X(\tau) &= \sum_{j=1}^{N} d_j\omega_j(x_{j0} + d_j\omega_j^2 X_0)\cos\omega_j\tau + \\ &+ \sum_{j=1}^{N} d_j\omega_j p_{j0}\sin\omega_j\tau - \\ &- \sum_{j=1}^{N} d_j\omega_j^2 p_{j0}\sin\left(\sum_{j=1}^{N}\frac{d_j^2\omega_j\tau}{2}+\tau\right) \\ &+ \left(X_0 - \sum_{j=1}^{N} d_j\omega_j x_{j0} - \sum_{j=1}^{N} d_j^2\omega_j^3 X_0\right)\times \\ &\times\cos\left(\sum_{j=1}^{N}\frac{d_j^2\omega_j\tau}{2}+\tau\right). \end{aligned} \tag{9}$$

The accuracy of the last expression is considerably greater than the solution of the regular perturbation theory given in Eq. (6) – this is illustrated in Fig. 1.

Next, we averaged the squared displacement of the system oscillator's coordinate, $D(\tau) = (X(\tau) - X_0)^2$, over the initial coordinates and momenta of the bath modes,

$$\begin{aligned} \langle D(\tau)\rangle &= \langle (X(\tau)-X_0)^2\rangle = \\ &= \frac{1}{Z}\int_{-\infty}^{+\infty}\mathrm{d}\vec{x}_0\int_{-\infty}^{+\infty}\mathrm{d}\vec{p}_0 (X(\tau)-X_0)^2\times \\ &\times\exp\left(-\beta\sum_{j=1}^{N} H_{j0}\right), \end{aligned} \tag{10}$$

where we have introduced the dimensionless inverse temperature $\beta = \hbar\Omega/(k_B T)$. Here $H_{j0} = \frac{\omega_j}{2}(p_{j0}^2 + x_{j0}^2)$ and $Z = \int_{-\infty}^{+\infty}\mathrm{d}\vec{x}_0\int_{-\infty}^{+\infty}\mathrm{d}\vec{p}_0\exp\left(-\beta\sum_{j=1}^{N} H_{j0}\right)$ is the partition function of the bath. The integrals are over all the coordinates and momenta of the bath oscillators. Thus, we obtain

$$\begin{aligned} \langle D(\tau)\rangle &= \left\{\left(X_0 - \sum_{j=1}^{N} d_j\omega_j^3 X_0\right)\cos(\lambda\tau+\tau) + \right. \\ &\left. + \sum_{j=1}^{N} d_j\omega_j^3 X_0\cos\omega_j\tau - X_0\right\}^2 + \\ &+ \sum_{j=1}^{N}\frac{d_j^2\omega_j}{\beta}\{\cos\omega_j\tau - \cos(\lambda\tau+\tau)\}^2 \\ &+ \sum_{j=1}^{N}\frac{d_j^2\omega_j}{\beta}\{\sin\omega_j\tau - \omega_j\sin(\lambda\tau+\tau)\}^2. \end{aligned} \tag{11}$$

Here we used the definition of the reorganization energy $\lambda = \sum_{j=1}^{N}\omega_j d_j^2/2$. This is the final expression for the $\langle D(\tau)\rangle$ obtained using the method of multiple scales.

The goal of our paper is to investigate the applicability of the frozen-modes approximation. Therefore, in the next step we assume that N_{frozen} bath modes are frozen, which in essence means that their coordinates and momenta do not change in time. Thus, the total number of modes is $N_{\text{frozen}} + N_{\text{fast}} = N$. For the notational clarity we renamed the interaction coefficients of

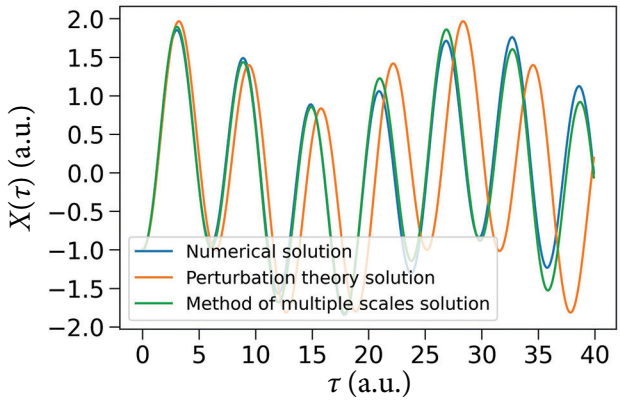

Fig. 1. Comparison of the exact numerical solution of the time-dependence of the coordinate of the main oscillator and solutions obtained using the regular perturbation theory (Eq. (6)) and the method of multiple scales (Eq. (9)). Here $N = 5$, $X_0 = -1$, $\omega_j = 0.25$, $d_j = 0.3$, $x_{j0} = 1$, $p_{j0} = 1$.

the frozen modes from d_j to g_j and once again applied the method of multiple scales to solve the system of equations given in Eq. (5), which transforms to

$$\begin{cases} \ddot{X} + X + \sum_{k=1}^{N_{\text{frozen}}} g_k^2 \omega_k X + \\ + \sum_{j=1}^{N_{\text{fast}}} d_j^2 \omega_j X - \sum_{k=1}^{N_{\text{frozen}}} g_k \omega_k x_{k0} - \sum_{j=1}^{N_{\text{fast}}} d_j \omega_j x_j = 0; \\ \ddot{x}_j + \omega_j^2 x_j - d_j \omega_j^2 X = 0. \end{cases} \tag{12}$$

As a result, the following expression was obtained:

$$\begin{aligned} \langle D(\tau)\rangle = & \left\{ \left(X_0 - \sum_{j=1}^{N_{\text{fast}}} \frac{d_j^2 \omega_j^3 X_0}{W^4} \right) \cos\left(\frac{\lambda_{\text{fast}} \tau}{W} + W\tau \right) + \right. \\ & \left. + \sum_{j=1}^{N_{\text{fast}}} \frac{d_j^2 \omega_j^3 X_0}{W^4} \cos \omega_j \tau - X_0 \right\}^2 + \\ & + \frac{2\lambda_{\text{slow}}}{\beta} \left\{ \left(-\frac{1}{W^2} + \sum_{j=1}^{N_{\text{fast}}} \left(\frac{d_j^2 \omega_j^3}{W^6} + \frac{d_j^2 \omega_j}{W^4} \right) \right) \times \right. \\ & \times \cos\left(\frac{\lambda_{\text{fast}} \tau}{W} + W\tau \right) - \sum_{j=1}^{N_{\text{fast}}} \left(\frac{d_j^2 \omega_j^3}{W^6} + \frac{d_j^2 \omega_j}{W^4} \right) \times \\ & \left. \times \cos \omega_j \tau + \frac{1}{W^2} \right\}^2 + \\ & + \sum_{j=1}^{N_{\text{fast}}} \frac{d_j^2 \omega_j}{\beta W^4} \left\{ \cos \omega_j \tau - \cos\left(\frac{\lambda_{\text{fast}} \tau}{W} + W\tau \right) \right\}^2 \\ & + \sum_{j=1}^{N_{\text{fast}}} \frac{d_j^2 \omega_j}{\beta W^4} \left\{ \sin \omega_j \tau - \frac{\omega_j}{W} \sin\left(\frac{\lambda_{\text{fast}} \tau}{W} + W\tau \right) \right\}^2 . \end{aligned} \tag{13}$$

Here λ_{slow} and λ_{fast} are defined as the reorganization energies for slow and fast modes, respectively, and $W = \sqrt{1 + 2\lambda_{\text{slow}}}$. This last expression was used in further numerical calculations, and it is one of the main results of the present paper. Moreover, it can be rewritten in terms of the dimensionless spectral density as

$$\begin{aligned} \langle D(\tau)\rangle = & \left\{ \left(X_0 - \frac{2X_0}{\pi W^4} \int_0^\infty \mathrm{d}\omega I_{\text{fast}}(\omega) \omega \right) \times \right. \\ & \times \cos\left(\frac{\lambda_{\text{fast}} \tau}{W} + W\tau \right) + \\ & \left. + \frac{2X_0}{\pi W^4} \int_0^\infty \mathrm{d}\omega \, I_{\text{fast}}(\omega) \omega \cos \omega\tau - X_0 \right\}^2 + \\ & + \frac{2\lambda_{\text{slow}}}{\beta} \left\{ \left(-\frac{1}{W^2} + \frac{2\int_0^\infty \mathrm{d}\omega' I_{\text{fast}}(\omega')\omega'}{\pi W^6} + \frac{2\lambda_{\text{fast}}}{W^4} \right) \times \right. \end{aligned} \tag{14}$$

(Eq. (14) continued)

$$\begin{aligned} & \times \cos\left(\frac{\lambda_{\text{fast}} \tau}{W} + W\tau \right) - \\ & - \frac{2}{\pi W^4} \int_0^\infty \mathrm{d}\omega' I_{\text{fast}}(\omega') \left(\frac{\omega'}{W^2} + \frac{1}{\omega'} \right) \cos \omega'\tau + \frac{1}{W^2} \Bigg\}^2 + \\ & + \frac{2}{\beta\pi W^4} \int_0^\infty \mathrm{d}\omega \frac{I_{\text{fast}}(\omega)}{\omega} \left\{ \cos \omega\tau - \cos\left(\frac{\lambda_{\text{fast}} \tau}{W} + W\tau \right) \right\}^2 + \\ & + \frac{2}{\beta\pi W^4} \int_0^\infty \mathrm{d}\omega \frac{I_{\text{fast}}(\omega)}{\omega} \left\{ \sin \omega\tau - \frac{\omega}{W} \sin\left(\frac{\lambda_{\text{fast}} \tau}{W} + W\tau \right) \right\}^2 . \end{aligned}$$

The mode-freezing approximation is expected to improve the accuracy of the pure multiple-scales solution at least in some parameter regimes, because the interaction coefficients of the frozen modes are included non-perturbatively to all orders.

3. Results

The system of equations given in Eq. (5) was numerically solved in Python with the Scipy.integrate package using the ODEINT function. To obtain the initial conditions and numerically estimate the value of the integral in Eq. (10), we used the Monte Carlo method, with the initial conditions for the bath oscillators being sampled from the Gaussian distribution. We have discretized the bath into 200 modes. This number of modes was sufficient for convergence since the results do not change if the number of modes is increased. The frequencies of the bath were defined as $\omega_j = j \cdot \Delta\omega$. Here $\Delta\omega = \omega_{\text{max}}/N$ and ω_{max} is the maximum frequency of the bath, that was chosen according to the cut-off frequency ω_c such that the condition $\omega_j < 1$ holds for all $j = 1, 2, ..., N$. This implies that the considered values of the cut-off frequency ω_c must be chosen in such a way that $\omega_{\text{max}} < 1$. Let us now define the parameters d_j. Having in mind the frequency dependence of the spectral density function in Eq. (2), we can define the unnormalized interaction coefficients as $\tilde{d}_j = \sqrt{I(\omega_j)/\omega_j^2}$, where $I(\omega_j)$ is the chosen spectral density function evaluated at ω_j. In order to properly normalize the interaction coefficients, we use the definition of reorganization energy:

$$\lambda = \frac{\lambda}{\sum_{k=1}^{N} \tilde{d}_k^2 \omega_k / 2} \cdot \sum_{j=1}^{N} \frac{\tilde{d}_j^2 \omega_j}{2} = \sum_{j=1}^{N} \frac{d_j^2 \omega_j}{2}. \tag{15}$$

Collecting terms next to every ω_j gives $\left(2\lambda / \sum_{k=1}^{N} \tilde{d}_k^2 \omega_k\right) \tilde{d}_j^2 = d_j^2$. Substituting $\tilde{d}_j = \sqrt{I(\omega_j)/\omega_j^2}$, and taking the square root we find that the normalized interaction coefficients are given by

$$d_j = \sqrt{\frac{2\lambda I(\omega_j)}{\omega_j^2 \sum_{k=1}^{N} I(\omega_k)/\omega_k}}. \tag{16}$$

For the MC averaging we used 2000 realizations, as increasing the number of realizations further barely changes the results. Note that for all calculations we set X_0 to 0, which simplifies the analysis. In addition, in such a case $\langle D(\tau)\rangle \sim 1/\beta$, thus the β parameter just sets the overall scale of $\langle D(\tau)\rangle$. The behaviour of the system is then determined only by two parameters of the spectral density, λ and ω_c.

To separate the high-frequency (fast) and the low-frequency (slow) modes, we used a splitting function $S(\omega, \omega^*)$. Thus, the spectral density is written as $I(\omega) = I_{\text{fast}}(\omega) + I_{\text{slow}}(\omega)$, where $I_{\text{slow}}(\omega) = S(\omega, \omega^*)\, I(\omega)$ and $I_{\text{fast}}(\omega) = (1 - S(\omega, \omega^*))\, I(\omega)$. Here the parameter ω^* controls how many of the bath modes will be frozen. We analyzed two splitting functions. First, following the literature [14–16, 24], we defined the splitting function as follows:

$$S(\omega, \omega^*) = \begin{cases} \left[1 - \left(\frac{\omega}{\omega^*}\right)^2\right]^2, & \omega < \omega^*; \\ 0, & \omega \geq \omega^*. \end{cases} \tag{17}$$

The second splitting function we analyzed was a simpler one:

$$S(\omega, \omega^*) = \theta(\omega^* - \omega). \tag{18}$$

This type of splitting essentially means that the spectral density is cut vertically and all the modes that have a frequency smaller than a certain chosen frequency ω^* are frozen, see illustration in Fig. 2. Even though the splitting function in Eq. (17) is being widely used in literature, no significant difference in the accuracy of the solutions was noticed for different splitting functions. Therefore, in further calculations the function in Eq. (18) was used owing to its simplicity.

The first point to consider is whether the frozen-modes approach indeed improves the accuracy of the multiple-scales solution. This is demonstrated in Fig. 3, which shows a comparison between the exact numerical results and the results obtained by using the method of multiple scales and the mode-freezing method. We observe that excellent accuracy can be obtained using the frozen-modes approximation. Similar improvements were observed for other parameter values, once a suitable value of ω^* is chosen. Indeed, the quality of the results strongly depends on the value of ω^*.

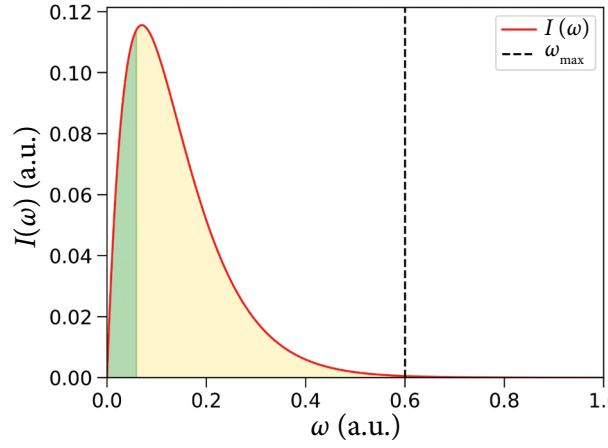

Fig. 2. Spectral density and its decomposition via rectangular splitting. All the low-frequency modes (green region) are frozen. Here $\omega_c = 0.07$, $\lambda = 0.1$, $\omega_{max} = 0.6$, $\omega^* = 0.06$.

For each specific parameter value set, there is a value ω^*_{best}, for which the most accurate results are obtained. The utility of the mode-freezing approach would be greatly increased, however, if a suitable value for ω^* could be identified *a priori*. After having analyzed numerous sets of parameters, we developed a simple rule for choosing the parameter ω^*, which was defined as follows:

$$\omega^* = \begin{cases} 0.03, & \lambda < 0.3, \\ 0.05, & \lambda \geq 0.3. \end{cases} \tag{19}$$

To illustrate the applicability of this rule, we analyzed various combinations of λ and ω_c values. Figures 4–6 show the results corresponding to ω_c equal to 0.035, 0.05 and 0.1, respectively. In all the calculations using the mode-freezing approximation, ω^* was selected based on the rule of Eq. (19).

Let us first consider the case of $\omega_c = 0.035$, which is demonstrated in Fig. 4. This corresponds to the slow bath regime – the system oscillator interacts mostly with the low-frequency

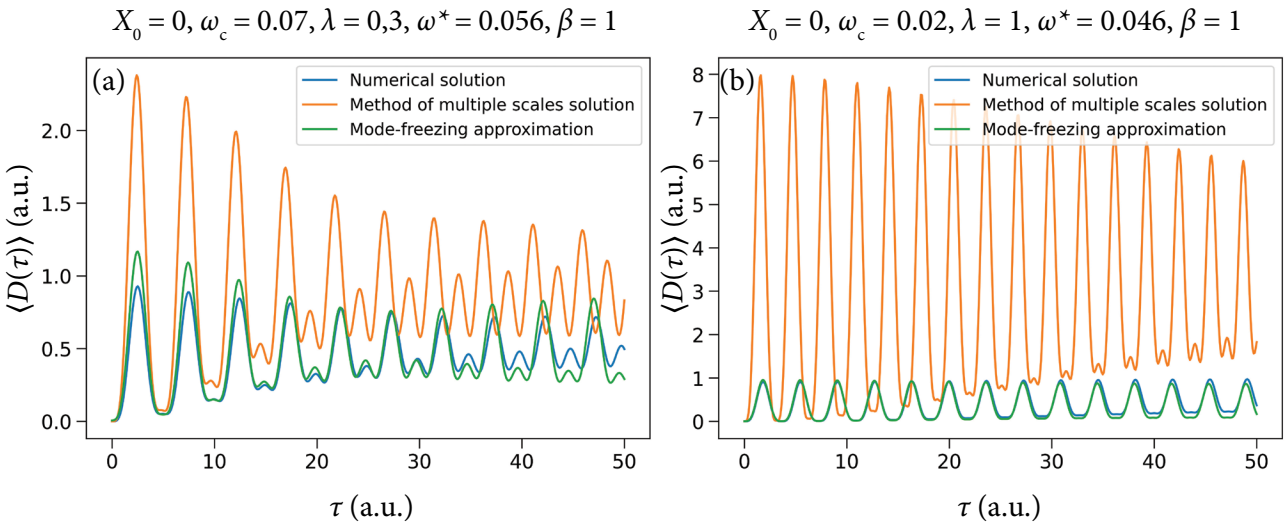

Fig. 3. Comparison of the exact numerical solution and solutions for $\langle D(\tau)\rangle$ obtained using the method of multiple scales (Eq. (11)) and the mode-freezing method (Eq. (13)) for two parameter value sets.

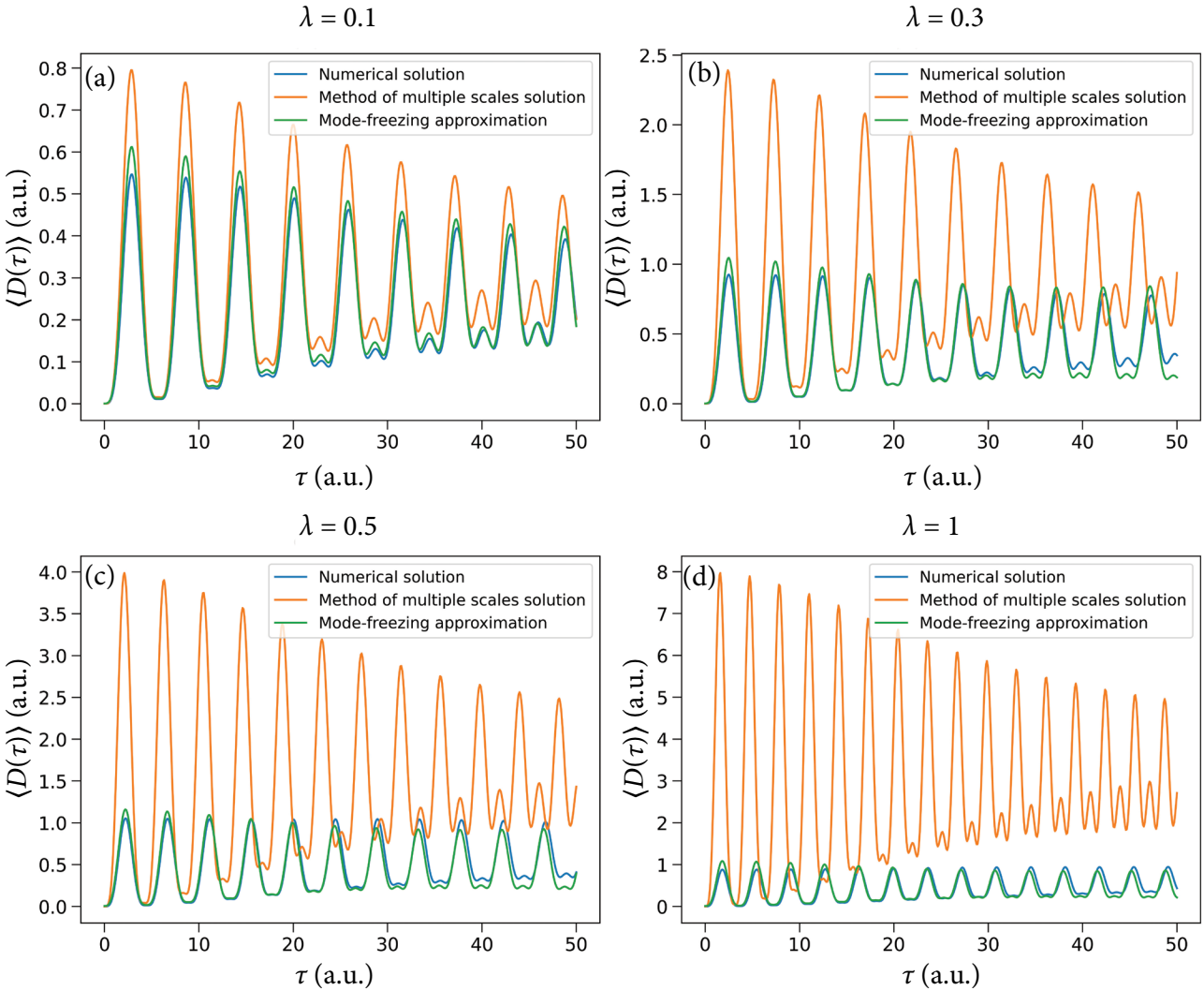

Fig. 4. Comparison of the exact numerical solution and solutions for $\langle D(\tau)\rangle$ obtained using the method of multiple scales (Eq. (11)) and the mode-freezing method (Eq. (13)). Here $X_0 = 0$, $\omega_c = 0.035$, $\beta = 1$, $\omega_{max} = 0.3$.

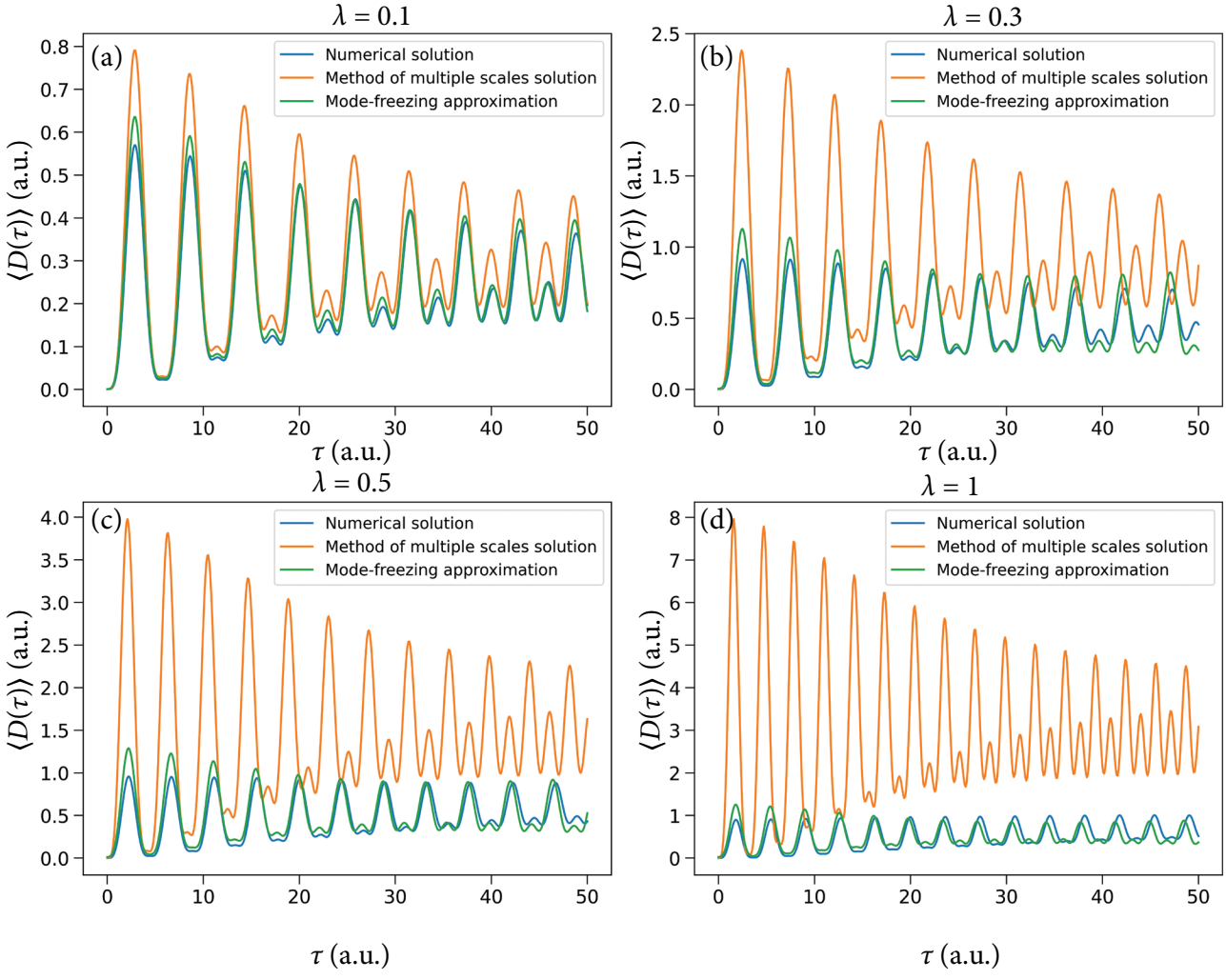

Fig. 5. Comparison of the exact numerical solution and solutions for $\langle D(\tau)\rangle$ obtained using the method of multiple scales (Eq. (11)) and the mode-freezing method (Eq. (13)). Here $X_0 = 0$, $\omega_c = 0.05$, $\beta = 1$, $\omega_{max} = 0.4$.

bath modes. For small reorganization energies ($\lambda = 0.1$), the method of multiple scales provides a reasonable accurate solution. However, it overestimates the amplitude of the oscillations. On the other hand, the mode-freezing approximation provides an excellent accuracy, since its solution is barely distinguishable from the exact numerical solution. As the reorganization energy increases, the accuracy of the method of multiple scales overestimates the amplitude of the oscillations even more. Application of the frozen modes approach results in a very good accuracy for all considered λ values, but the accuracy decreases slightly as λ increases.

Next, we consider the case of a slightly faster bath with $\omega_c = 0.05$, which is illustrated in Fig. 5. It can be seen that a faster bath results in a somewhat faster decay of the oscillation amplitude for $\langle D(\tau)\rangle$. The method of multiple scales results in a solution that is reasonably accurate only for the smallest considered reorganization energy value. The larger the reorganization energy is, the more this approach overestimates the amplitude of the oscillations. The frozen-modes approach gives accurate results for all considered reorganization energies. Nonetheless, it can be observed that it is slightly less accurate than in the case of slower bath.

Finally, we will consider the case of an even faster bath with $\omega_c = 0.1$, shown in Fig. 6. The overall tendencies are similar to the cases of slower bath. In this case, however, the frozen-modes approach no longer gives an excellent accuracy when the reorganization energy is large (see Fig. 6(c, d)). Nonetheless, it is still considerably more accurate than the method of multiple scales.

For the sake of simplicity, in Figs. 3–6 we set the initial coordinate of the main oscillator to be

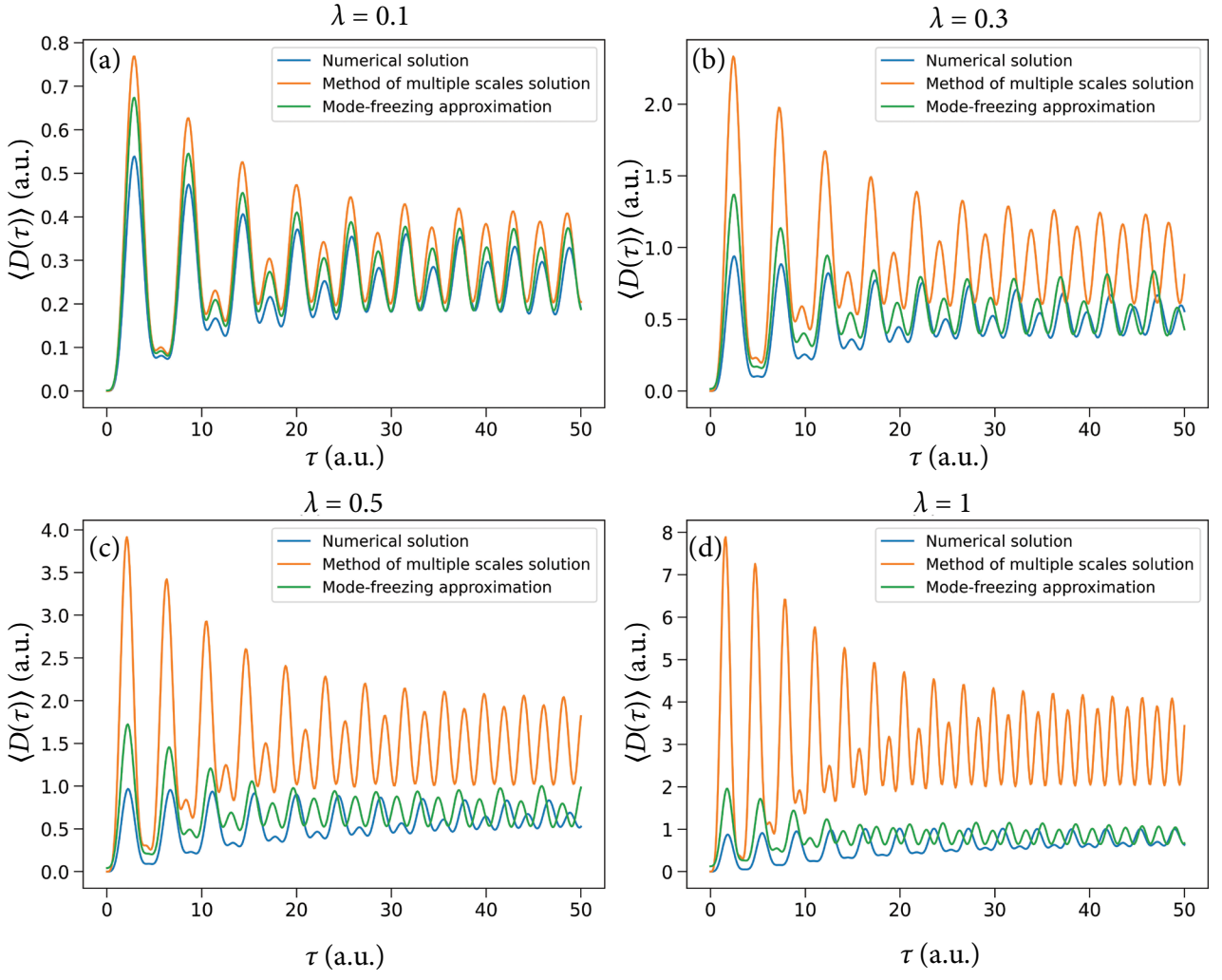

Fig. 6. Comparison of the exact numerical solution and solutions for $\langle D(\tau)\rangle$ obtained using the method of multiple scales (Eq. (11)) and the mode-freezing method (Eq. (13)). Here $X_0 = 0$, $\omega_c = 0.1$, $\beta = 1$, $\omega_{max} = 0.8$.

equal to zero. However, the frozen-modes approach not only gives accurate results for $X_0 = 0$ but also for any other value of X_0, see Fig. 7. For small values of λ both the method of multiple scales and the frozen-modes approximation gives excellent results as the blue, green and orange lines are almost indistinguishable. As the reorganization energy increases, the oscillation frequency of the solution of the method of multiple scales starts to differ from the frequencies of the exact numerical solution and the oscillation amplitude is overestimated. Meanwhile, the frozen-modes approximation gives significantly more accurate results than the method of multiple scales even for large λ values.

Although we have mostly focused on the ohmic spectral density (Eq. (3)), it is interesting to see if our results can be generalized. Thus, a few other forms of the spectral density were analyzed, albeit in less detail. Using the super-ohmic spectral density defined as

$$I(\omega) = \frac{\pi\lambda}{2}\left(\frac{\omega}{\omega_c}\right)^3 \exp\left(-\frac{\omega}{\omega_c}\right), \tag{20}$$

the frozen-modes approach results in a good accuracy for small values of parameter ω_c (not shown). As can be seen in Fig. 8, when ω_c is increased, the accuracy is worse not only for the rule of Eq. (19), but also for the best possible choice of ω^*.

A similar situation was observed in the case of the spectral density defined as

$$I(\omega) = \frac{2\sqrt{\pi}\lambda\omega}{\omega_c}\exp\left[-\left(\frac{\omega}{\omega_c}\right)^2\right]. \tag{21}$$

It is illustrated in Fig. 9 that for large ω_c values the rule of Eq. (19) does not result in an accurate

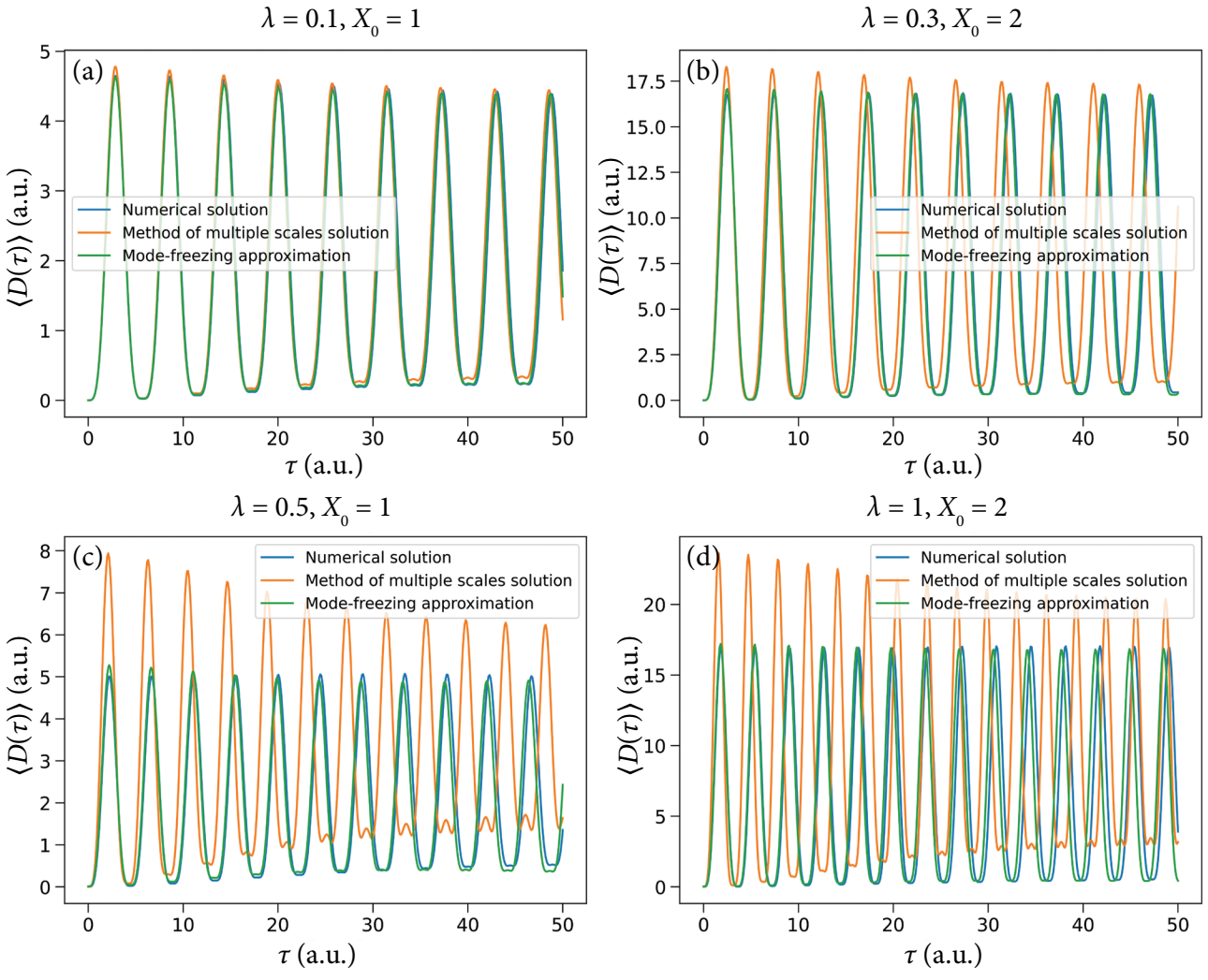

Fig. 7. Comparison of the exact numerical solution and solutions for $\langle D(\tau)\rangle$ obtained using the method of multiple scales (Eq. (11)) and the mode-freezing method (Eq. (13)) when $X_0 \neq 0$. Here $\omega_c = 0.05$, $\beta = 1$, $\omega_{max} = 0.4$.

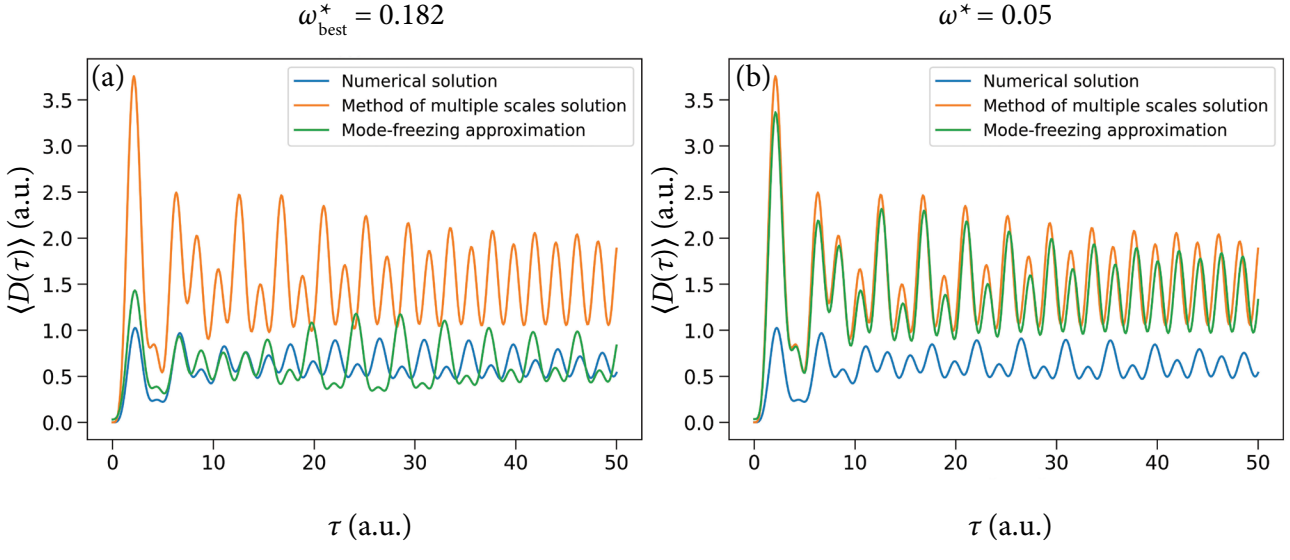

Fig. 8. Results for $\langle D(\tau)\rangle$ in the case of super-ohmic spectral density (Eq. (20)) when choosing the best ω^* (left) and choosing ω^* according to the rule of Eq. (19) (right). Here $X_0 = 0$, $\omega_c = 0.07$, $\lambda = 0.5$, $\beta = 1$, $\omega_{max} = 0.8$.

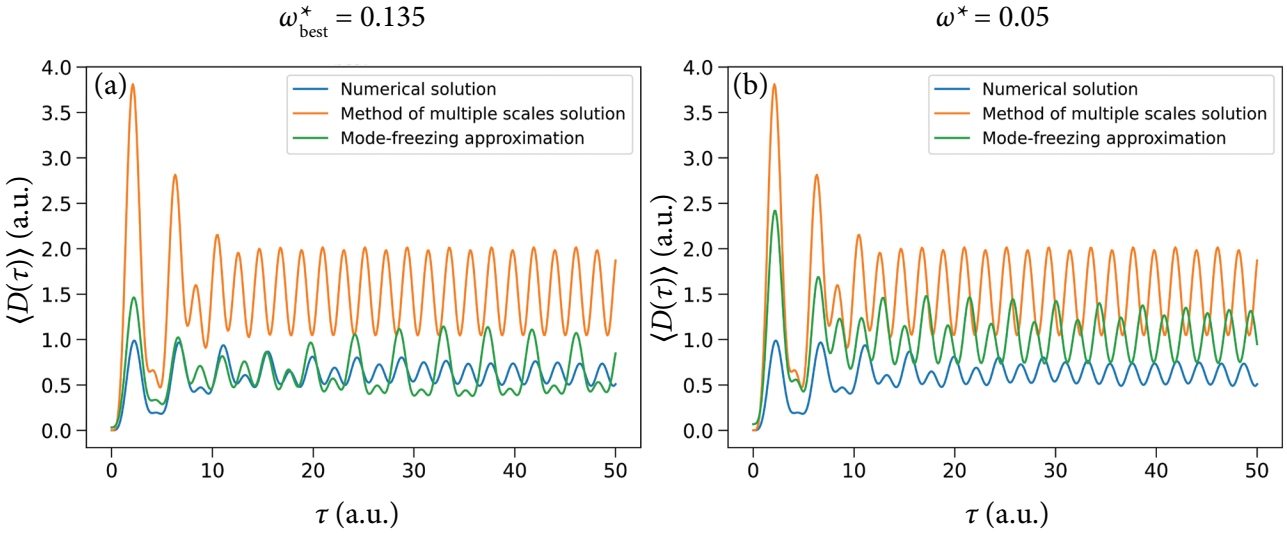

Fig. 9. Results for $\langle D(\tau)\rangle$ in the case of the spectral density of Eq. (21) when choosing the best ω^* (left) and choosing ω^* according to the rule of Eq. (19) (right). Here $X_0 = 0$, $\omega_c = 0.3$, $\lambda = 0.5$, $\beta = 1$, $\omega_{\text{max}} = 0.8$.

solution using the frozen-modes approach. Using the ω^*_{best} gives somewhat more accurate results, which are still worse than for the ohmic spectral density.

On the other hand, if we consider a spectral density defined as

$$I(\omega) = \frac{\pi\lambda\omega}{2\omega_c}\exp\left(-\sqrt{\frac{\omega}{\omega_c}}\right), \tag{22}$$

quite accurate results can be achieved for all values of ω_c for both choosing the best ω^* and using the rule of Eq. (19), as illustrated in Fig. 10.

It must be noted, however, that a comparison of different spectral densities is not straightforward. Due to different functional forms, different numerical values of the cut-off frequency ω_c must be used to guarantee that the spectral densities decay enough for ω values approaching 1, which is the limit considered in this work. This is the reason for the at first glance surprising results that better accuracy using the frozen-modes approximation can be obtained for the spectral density that decays slower (see Fig 10) than for the spectral density that decays faster (see Fig. 9) for larger ω_c values.

4. Discussion

In this work, we have investigated the application of the frozen-modes approximation to the classical

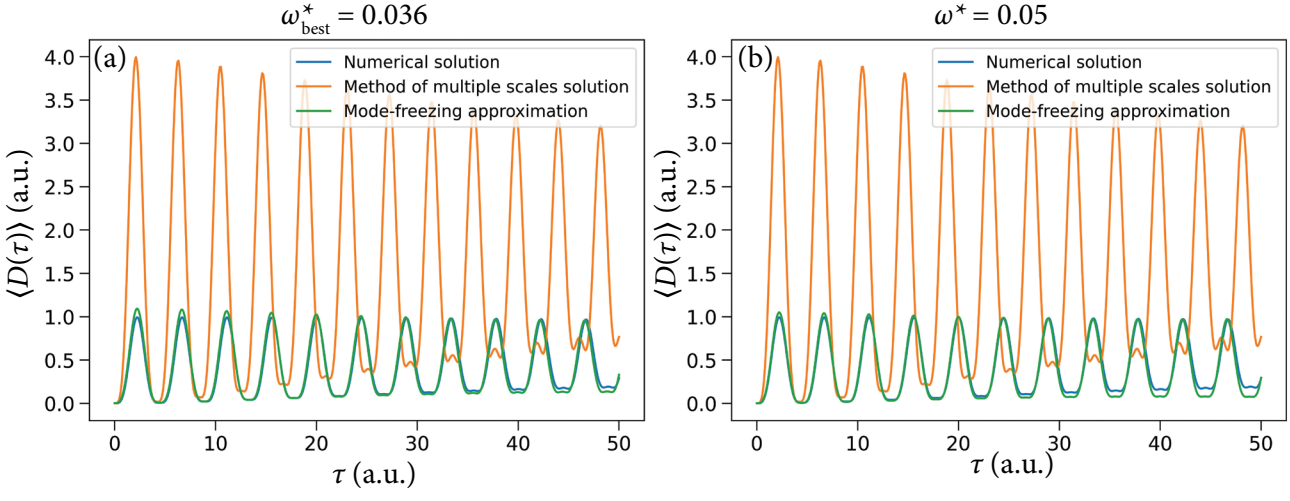

Fig. 10. Results for $\langle D(\tau)\rangle$ in the case of the spectral density of Eq. (22) when choosing the best ω^* (left) and choosing ω^* according to the rule of Eq. (19) (right). Here $X_0 = 0$, $\omega_c = 0.003$, $\lambda = 0.5$, $\beta = 1$, $\omega_{\text{max}} = 0.6$.

harmonic oscillator systems. Our results show that it can increase the accuracy of the solution obtained from the method of multiple scales significantly. Now we would like to discuss the applicability of the present approach and general considerations arising from its application.

The first point is that the frozen-modes approximation is justified only for slow baths. Physically, the freezing of the bath modes can be expected not to influence the dynamics of the system oscillator if the coordinates and momenta of these modes barely change in the time interval under consideration. For this to be the case, the frequency of such modes have to be much smaller than the characteristic frequency of the system motion. Here we have restricted our consideration to this limit by analyzing only the spectral densities that decay to zero for frequencies approaching the frequency of the system oscillator. For such situations the frozen-modes approximation can provide very accurate results even for very large reorganization energy values (see Fig. 4(d)), which would not be possible by straightforward applications of the perturbative approaches. For faster baths, however, the accuracy of this approach decreases, even though it remains much more accurate than the method of multiple scales (see Fig. 6(d)).

The application of the frozen-modes approach involves choosing a value for ω^*, which determines the splitting of the spectral density to fast and slow modes. For $\omega^* \to 0$, the solution of the multiple-scales method is recovered, while for $\omega^* \to \infty$ all the bath modes are frozen. The accuracy of the frozen-modes approach is strongly dependent on a suitable choice of ω^*. In this work, we investigated the choices for ω^*, but this required the availability of the exact solution. If such a solution is not available, it is not possible to select the value of ω^* without any additional considerations. Therefore, we suggested a simple rule of selecting this value that is given in Eq. (19). For the ohmic spectral density that was mostly considered here, this rule resulted in a very good accuracy for the frozen-modes solution in most cases. Such types of rules were also suggested in the application of the frozen-modes approach for open quantum systems [14–16].

It must be noted that the requirement that the bath frequencies should not approach the frequency of the system oscillator limits the possible types of spectral densities, for which the present approach could be useful. Another point to consider is that the super-ohmic spectral densities also lead to less accurate solutions, because of small couplings with the low-frequency bath modes (see Fig. 8).

It is also worthwhile to consider the full frozen-modes limit when all the bath modes are frozen. In such a case, the expression for $\langle D(\tau)\rangle$ reduces to

$$\langle D(\tau)\rangle = \left(X_0^2 + \frac{2\lambda}{\beta(1+2\lambda)^2} \right) \times \times \left[1 - \cos\left(\sqrt{1+2\lambda}\,\tau \right) \right]^2 . \tag{23}$$

Two main points are of interest here. The first one is that the solution oscillates only with a single frequency $\sqrt{1+2\lambda}$ (and its second harmonic), which represents the renormalized frequency of the main oscillator. The second one is that the oscillation amplitude remains constant in time. This means that there is no energy exchange between the system and the bath, and thus no relaxation or thermalization effects.

Another interesting point is that the mode-freezing approximation is postulated in an *ad hoc* manner. To analytically motivate the mode-freezing approximation, we have applied the method of multiple scales for the system of equations given in Eq. (5), supposing that the frequencies ω_j, rather than the couplings d_j, are multiplied by a small parameter ε. This essentially means that the frequencies of the bath modes are much smaller than the frequency of the main oscillator and thus should correspond to the frozen-modes limit. Consequently, the following second-order solution was obtained:

$$\begin{aligned} X(\tau) = {} & \left(X_0 - \sum_{j=1}^{N} d_j \omega_j x_{j0} + 2\sum_{j=1}^{N} d_j \omega_j x_{j0} \lambda \right) \times \\ & \times \cos\left(\lambda\tau - \frac{1}{2}\lambda^2\tau + \tau \right) - \\ & - \sum_{j=1}^{N} d_j \omega_j^2 p_{j0} \sin\left(\lambda\tau - \frac{1}{2}\lambda^2\tau + \tau \right) + \\ & + \sum_{j=1}^{N} d_j \omega_j (\omega_j p_{j0}\tau + x_{j0}) - \\ & - 2\lambda \sum_{j=1}^{N} d_j \omega_j x_{j0} . \end{aligned} \tag{24}$$

As can be seen, terms that are proportional to time τ appear, thus the solution diverges when time goes

to infinity. Therefore, this type of approach does not allow us to recover the frozen-modes approximation.

Finally, let us discuss the more general applicability of the frozen-modes approximation. Clearly, analytical solutions are possible only for the harmonic potentials of the system. Nonetheless, it is possible to apply the frozen modes approach even for non-harmonic potentials. This could be done when solving the resulting system of equations numerically. When the bath is discretized, the lowest frequency modes could be frozen, thus reducing the number of dynamical variables. It must be noted that this makes sense only when using the rectangular splitting of the spectral density. Indeed, using the splitting function given in Eq. (17) would not result in a reduction of bath modes needed to be included explicitly in the calculations. For the rectangular splitting of the spectral density, a comparison of the exact numerical solution for $\langle D(\tau)\rangle$ and the numerical solution when the low-frequency modes are frozen is shown in Fig. 11. In the numerical solution with frozen modes, the coordinates and momenta of the oscillators with frequencies lower than $\omega^* = 0.05$ are treated as constants (taken from the Gaussian distribution), while the rest are dynamical variables. As can be observed, the oscillation amplitude of the exact solution decays faster than the one of the solution with frozen modes.

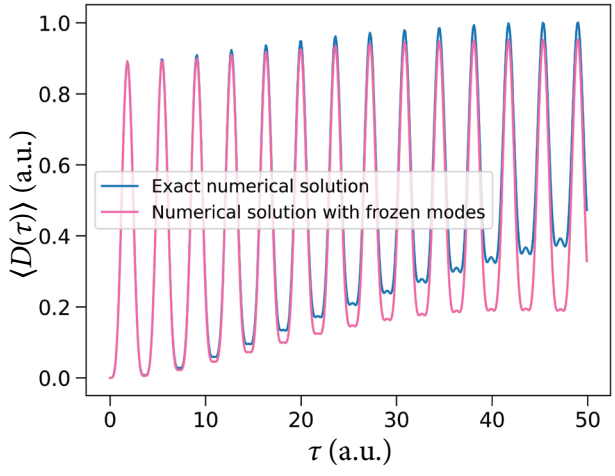

Fig. 11. Comparison of the exact numerical solution for $\langle D(\tau)\rangle$ and the numerical solution when the low frequency modes are frozen. Here $\omega_{max} = 0.3$ and $\omega^* = 0.05$, therefore, 17% of the modes are frozen. Other parameters: $X_0 = 0$, $\lambda = 1$, $\omega_c = 0.035$, $\beta = 1$.

However, the numerical solution with frozen low-frequency modes has a lower computational cost than the exact one. Therefore, the frozen-modes approximation provides a controllable trade-off between the accuracy and the computational cost.

5. Conclusions

In this paper, we investigated the applicability of the frozen-modes approximation to the classical harmonic oscillator systems. Our results show that for slow baths, freezing some of the bath modes can increase the accuracy of the perturbative multiple-scales solution significantly. For faster baths, the frozen-modes solution is less accurate, but it remains more accurate than the pure multiple-scales solution. To facilitate the applicability of the frozen-modes approach, we devised a rule for splitting the spectral density into slow modes that are frozen and fast modes that are not. While we have mostly focused on the ohmic spectral density, this approach could be useful for other similar spectral densities as well. For super-ohmic spectral densities, however, the frozen-modes approach does not provide a considerable gain in accuracy. Finally, we have suggested that the frozen modes approach could also be useful for numerical simulations, as it provides a controllable trade-off between accuracy and computational cost. We believe that our contribution will stimulate the application of the frozen-modes approximation to the classical oscillator systems.

Acknowledgements

This work was supported by the Research Council of Lithuania (LMT Grant No. S-MIP-23-31).

References

[1] H.-P. Breuer and F. Petruccione, *The Theory of Open Quantum Systems* (Oxford University Press, 2002).

[2] U. Weiss, *Quantum Dissipative Systems* (World Scientific, 2008).

[3] I. de Vega and D. Alonso, Dynamics of non-Markovian open quantum systems, Rev. Mod. Phys. **89**, 015001 (2017).

[4] M. Razavy, *Classical and Quantum Dissipative Systems* (Imperial College Press, 2005).

[5] K. Zhou and B. Liu, *Molecular Dynamics Simulation: Fundamentals and Applications* (Elsevier, 2022).

[6] J.S. Bader and B.J. Berne, Quantum and classical relaxation rates from classical simulations, J. Chem. Phys. **100**, 8359 (1994).

[7] H. Hasegawa, Classical small systems coupled to finite baths, Phys. Rev. E **83**, 021104 (2011).

[8] A.O. Caldeira and A.J. Leggett, Quantum tunnelling in a dissipative system, Ann. Phys. **149**, 374 (1983).

[9] G.W. Ford and M. Kac, On the quantum Langevin equation, J. Stat. Phys. **46**, 803 (1987).

[10] H. Hasegawa, Responses to applied forces and the Jarzynski equality in classical oscillator systems coupled to finite baths: An exactly solvable nondissipative nonergodic model, Phys. Rev. E **84**, 011145 (2011).

[11] J.S. Briggs and A. Eisfeld, Coherent quantum states from classical oscillator amplitudes, Phys. Rev. A **85**, 052111 (2012).

[12] T.E. Skinner, Exact mapping of the quantum states in arbitrary *n*-level systems to the positions of classical coupled oscillators, Phys. Rev. A **88**, 012110 (2013).

[13] T. Mančal, Excitation energy transfer in a classical analogue of photosynthetic antennae, J. Phys. Chem. B **117**, 11282 (2013).

[14] A. Montoya-Castillo, T.C. Berkelbach, and D.R. Reichman, Extending the applicability of Redfield theories into highly non-Markovian regimes, J. Chem. Phys. **143**, 194108 (2015).

[15] J.H. Fetherolf and T.C. Berkelbach, Linear and nonlinear spectroscopy from quantum master equations, J. Chem. Phys. **147**, 244109 (2017).

[16] H.-H. Teh, B.-Y. Jin, and Y.-C. Cheng, Frozen-mode small polaron quantum master equation with variational bound for excitation energy transfer in molecular aggregates, J. Chem. Phys. **150**, 224110 (2019).

[17] A.A. Kananenka, C.-Y. Hsieh, J. Cao, and E. Geva, Accurate long-time mixed quantum-classical Liouville dynamics via the transfer tensor method, J. Phys. Chem. Lett. **7**, 4809 (2016).

[18] C. Chuang, D.I. Bennett, J.R. Caram, A. Aspuru-Guzik, M.G. Bawendi, and J. Cao, Generalized Kasha's model: *T*-dependent spectroscopy reveals short-range structures of 2d excitonic systems, Chem **5**, 3135 (2019).

[19] A. Gelzinis and L. Valkunas, Analytical derivation of equilibrium state for open quantum system, J. Chem. Phys. **152**, 051103 (2020).

[20] Y. Lai and E. Geva, On simulating the dynamics of electronic populations and coherences via quantum master equations based on treating off-diagonal electronic coupling terms as a small perturbation, J. Chem. Phys. **155**, 204101 (2021).

[21] J.G. Simmonds and J.E. Mann, *A First Look at Perturbation Theory* (Dover Publications, 1997).

[22] A.H. Nayfeh, *Introduction to Perturbation Techniques* (Wiley-VCH, 1981).

[23] M.H. Holmes, *Introduction to Perturbation Methods* (Springer, 1995).

[24] T.C. Berkelbach, D.R. Reichman, and T.E. Markland, Reduced density matrix hybrid approach: An efficient and accurate method for adiabatic and non-adiabatic quantum dynamics, J. Chem. Phys. **136**, 034113 (2012).

UŽŠALDYTŲ MODŲ ARTINIO TAIKYMAS KLASIKINIŲ HARMONINIŲ OSCILIATORIŲ SISTEMOMS

J. Vaičaitytė [a, b], L. Valkūnas [a], A. Gelžinis [a, b]

[a] *Fizinių ir technologijos mokslų centro Molekulinių darinių fizikos skyrius, Vilnius, Lietuva*

[b] *Vilniaus universiteto Fizikos fakulteto Cheminės fizikos institutas, Vilnius, Lietuva*

Santrauka

Atviruųjų klasikinių sistemų uždaviniai dažniausiai yra susiję su dalelės, sąveikaujančios su dideliu skaičiumi aplinkos osciliatorių, judėjimu. Gana dažnai nagrinėjama dalelė irgi gali būti laikoma harmoniniu osciliatoriumi. Tokių sistemų uždavinį galima skaitiškai išspręsti tiksliai, bet reikalingi skaičiavimo pajėgumai smarkiai auga didėjant aplinkos osciliatorių skaičiui. Pastaraisiais metais pasirodė darbų, kuriuose užšaldytų modų artinys buvo pritaikytas atvirosioms kvantinėms sistemoms. Šiame darbe mes pritaikome šį metodą atvirosioms klasikinėms sistemoms. Taikant šį artinį laikoma, kad dalis žemo dažnio aplinkos modų yra užšaldytos, todėl reikia įskaityti tik jų koordinačių ir judesio kiekių pradines vertes. Parodome, kad užšaldytų modų artinio taikymas gali gerokai praplėsti trikdžių teorija paremto daugelio skalių metodo taikymo ribas. Gaunamas geras tikslumas net esant stipriai sistemos osciliatoriaus sąveikai su aplinkos osciliatoriais, ką yra sunku pasiekti taikant įprastus artutinius metodus. Taip pat pasiūlome taisyklę, kaip padalinti aplinkos spektrinį tankį į greitas ir lėtas modas. Pasiūlytas metodas veikia itin gerai, kai sistema aprašoma ominio tipo spektriniu tankiu, bet jis yra tinkamas ir kitiems aplinkos modeliams.